FINITE ELEMENT ANALYSIS OF EDDY CURRENT SURFACE PROBES+

H. Hoshikawa
Nihon University, Tokyo, Japan
R. M. Li
Shanghai Research Institute, Shanghai, China
N. Ida
Colorado State University, Fort Collins, CO 80523

INTRODUCTION

Surface eddy current probes are widely used for measuring crack depth, coating thickness and corrosion effects in metals. In most applications, single (absolute) coils are used, and the coil impedance is monitored. Information concerning inhomogeneities is extracted from changes in the coils impedance. Double probes consist of a driving coil and a smaller concentric pickup coil. In this case the induced voltage in the pickup coil is measured. This work describes the application of the finite element method to the analysis and design of both single and double coil surface probes. Double coil probes are shown to be superior for the applications mentioned above because of better linearity of the lift off curve and wider useful range. The rate of change of the induced voltage in a double coil probe is shown to be larger than the rate of change of the impedance in single coil probes for given parameter changes. This clearly indicates a higher sensitivity. Moreover, in the case of corrosion depth measurement, the noise generated by lift off changes can be suppressed by use of an appropriate double coil. The results presented are also verified experimentally.

SINGLE AND DOUBLE COIL SURFACE PROBES

The different probes considered in this work are illustrated in Fig. 1 as they relate to lift off measurements. Fig. 1a

+This work has been sponsored by the Electric Power Research Institute.

represents a small diameter absolute coil over a conducting surface. Because of the localized nature of the probe fields, the range of lift off measurement is limited. A larger diameter coil such as the coil in Fig. 1b can extend this range, but a better sensitivity can be achieved by introducing a small diameter pickup coil at the center of the larger coil as in Fig. 1c. Because the flux lines through the pickup coil are essentially perpendicular to the conducting surface, the double coil probe should have better linearity and a wider useful range. These effects are clearly accentuated in Fig. 2 where the effect of a flat bottomed hole is shown. In Fig. 2a, there is little disturbance of the coils field due to the localized field pattern. In Fig. 2b, the large diameter of the coil tends to mask the hole signal because there is little change due to the hole, but a double coil has the advantage of both of the above as shown in Fig. 2c. Because the bottom of the hole affects the flux passing through the pickup coil, it should be possible to measure a wide range of hole depths.

THE FINITE ELEMENT MODEL

Details of the finite element model used in this study can be found in references 1 to 3. It consists of the discretization of

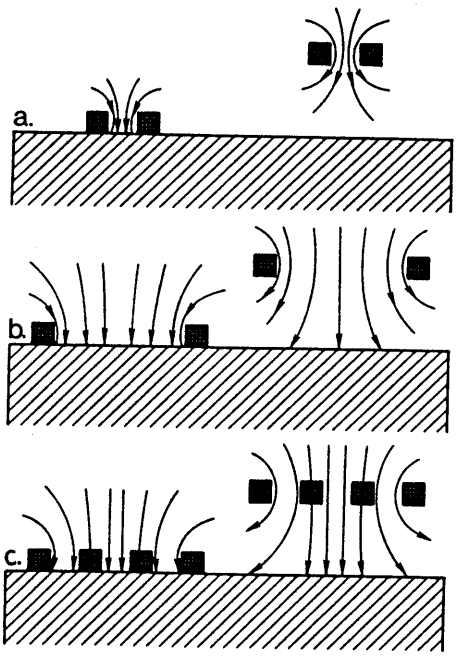

Fig. 1. Surface probes over a conducting surface. a) small diameter single coil, b) large diameter coil and c) double coil probe.

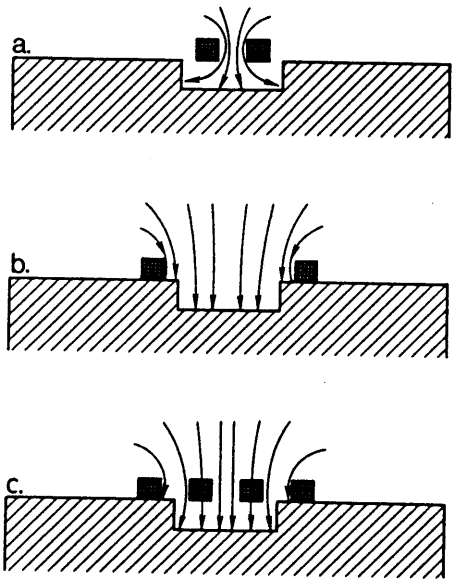

Fig. 2. Surface probes in the presence of flat bottomed holes. a) small diameter single coil, b) large diameter coil and c) double coil probe.

the solution region into finite elements (6000 elements and 3146 nodes were used), formulation of the field equation in an axisymmetric form and solution of the resulting system of linear equations to yield the magnetic vector potential at each node in the solution region. From the values of the magnetic vector potential the impedance of the coil can be calculated as[2]

$$\bar{Z} = \frac{j\omega 2\pi J_s}{I^2} \sum_{i=1}^{N_c} (r_{ci}\Delta_i)\bar{A}_{ci} \tag{1}$$

where ω is the angular frequency, J_s and I_s are the current density and current (RMS value) in the coil, N_c is the number of elements in the coil's cross section and r_{ci} is the distance of the centroid of element i from the axis of the coil. Δ_i represents the area of element i and A_{ci} is the complex centroidal value of the magnetic vector potential in element i. Similarly, the induced voltage in the small pickup coil can be calculated as

$$\bar{V} = -\oint_c \bar{E}.d\bar{\ell}. \tag{2}$$

For sinusoidal steady state excitation the induced voltage is

$$\bar{V} = j\omega \oint_c \bar{A}.d\ell \tag{3}$$

Noting that the induced voltage can be written as $\bar{V}=\bar{I}_r\bar{Z}$ where I_r is the RMS value of the induced current and taking the expression in Eq. (1) for Z, the induced voltage becomes

$$\bar{V} = \frac{j\omega 2\pi J_r}{I_r} \sum_{i=1}^{N_p} (r_{ci}\Delta_i)\bar{A}_{ci} \tag{4}$$

In this expression N_p is the number of elements in the cross section of the pickup coil. The induced current density (J_r) and therefore I_r are not known and the induced voltage cannot be calculated from this equation directly. In this application the normalized impedance and induced voltage are used. Normalizing the coil impedance with respect to $j\omega 2\pi J_s/I_s^2$ and the induced voltage with respect to $j\omega 2\pi J_r/I_r$, the two quantities have the same magnitude for identical coils and therefore are calculated as

$$\bar{Z}_n = \sum_{i=1}^{N_c} r_{ci}\Delta_i\bar{A}_{ci} \quad \text{and} \quad \bar{V}_n = \sum_{i=1}^{N_p} r_{ci}\Delta_i\bar{A}_{ci} \tag{5}$$

where the only difference is in the number of elements in each coil, their relative location (r_{ci}), their area (Δ_i) and the values of the magnetic vector potential A_{ci}. Both Z_n and V_n are complex values the subscript denoting normalized quantities.

RESULTS

The method described above was applied to three different absolute coils, 4, 10 and 30 mm in diameter and to a double coil probe consisting of an exciting coil, 30 mm in diameter and a small concentric pickup coil, 4 mm in diameter. In all cases the coil thickness is 3.9 mm. The performance of these probes was calculated for magnetic and nonmagnetic materials. The magnetic material used was carbon steel with conductivity equal to 5.10^6 [mho/m] and relative permebility of 50. The nonmagnetic material was Inconel 600 with a conductivity of $1.1.10^6$ [mho/m]. The magnetic material was tested at 1kHz and the nonmagnetic material at 10kHz. For each of the materials the lift off curves as well as curves resulting from depth changes in flat bottomed holes were obtained and compared. The excitation levels were assumed to be very small and therefore nonlinearities and hysteresis losses could be neglected.

LIFT OFF CALCULATIONS

Figs. 3 and 4 summarize the results obtained for the various probes with respect to lift off. The impedance change rate is plotted for the absolute probes and the rate of change of induced voltage is plotted for the double probe in Fig. 3. Z_0 and V_0 represent the probe impedance and induced voltage at zero lift off. Fig. 3a shows the rates of change of impedance and induced voltage due to lift off in the nonmagnetic material. The curve for the double probe indicates that its sensitivity for lift off changes is far larger than for any of the absolute probes. Fig. 3b shows similar calculations for carbon steel. The change in the induced voltage in the double probe occurs over a wider range of lift off values than

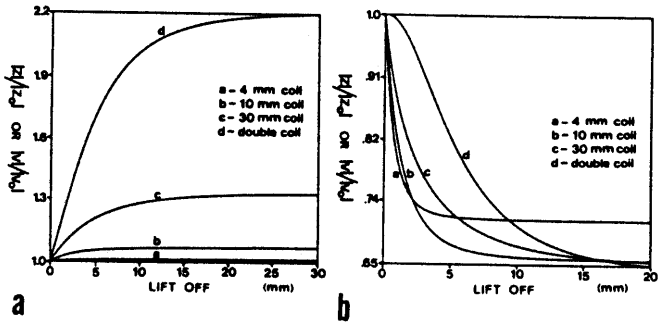

Fig. 3. Finite element predicted rates of change of impedance and induced voltage in surface probes due to changes in lift off. a) nonmagnetic material and b) magnetic material.

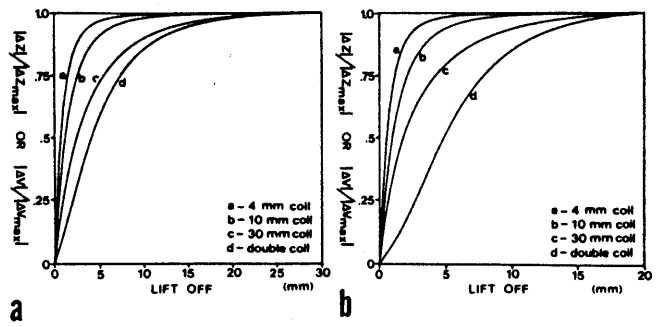

Fig. 4. Normalized rates of change of impedance and induced voltage due to lift off changes. a) nonmagnetic material and b) magnetic material.

for the absolute probes. To clarify the differences in range and linearity of lift off calculations between the various probes, the normalized curves in Fig. 4 are useful. Here, the change in the impedance defined as $\Delta Z = Z - Z_0$ is normalized with respect to ΔZ_{max} which is defined as $\Delta Z_{max} = Z_\infty - Z_0$. Z_∞ is the impedance of the coil at infinite lift off. Similarly, the change in the induced voltage is normalized with respect to ΔV_{max}. The normalized rates of change are defined as $\Delta Z/\Delta Z_{max}$ and $\Delta V/\Delta V_{max}$. The useful range for lift off measurement is larger and with better linearity than for the ansolute probes for the magnetic material (Fig 4b) and the nonmagnetic material (Fig. 4a).

HOLE DEPTH CALCULATIONS

To simulate a situation where the depth of a discontinuity in the metal such as corrosion is to be evaluated, flat bottomed holes of various diameters were used in conjunction with the probed described in the previous section. In this case, the probe was located over the hole, flush with the metal's surface and centralized with the hole. The hole depth was then changed and the signal from the probe plotted. Fig. 5 shows the rate of change of impedance or induced voltage due to the change in depth of a 10 mm diameter hole. Similarly, Fig. 6 represents the normalized rates of change for the same situation. Again, the sensitivity, useful range and linearity are better in the case of the double probe.

NOISE SUPPRESSION CHARACTERISTICS

When eddy current probes are used for such applications as crack and corrosion detection, the noise due to lift off variations needs to be suppressed. The most common method for lift off suppression is the phase discrimination method which uses the phase difference between the signal and noise. This method works best when the phase difference is close to 90° but is of little use if phase difference between the signal and the lift off signal is small. Fig. 7a

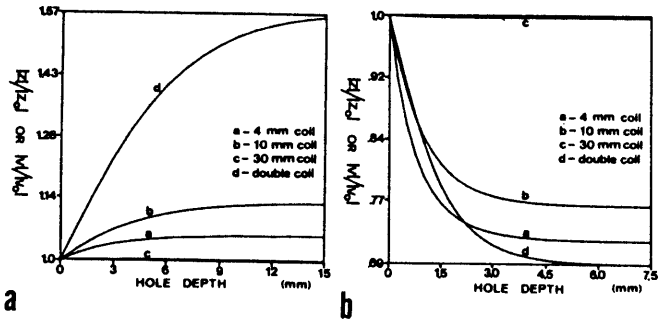

Fig. 5. Predicted change rates of impedance and induced voltage due to hole depth change. a) nonmagnetic material and b) magnetic material. (Hole diameter: 10 mm)

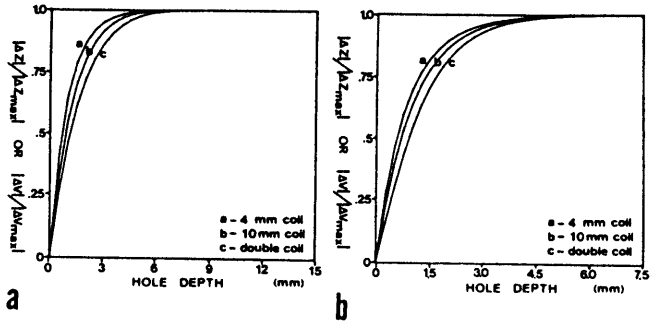

Fig. 6. Normalized change rates of impedance and induced voltage due to hole depth changes. a) nonmagnetic material and b) magnetic material. (Hole diameter: 10 mm).

shows the normalized impedance of a 4 mm diameter single coil probe in the case of a magnetic material. The phase between the hole depth change signal is very small and consequently, noise suppression is difficult in this situation. Fig. 7b shows the normalized induced voltage of a double coil probe for the same situation as in Fig. 7a. It is clear that the phase difference is significantly larger and therefore, noise suppression can be performed successfully.

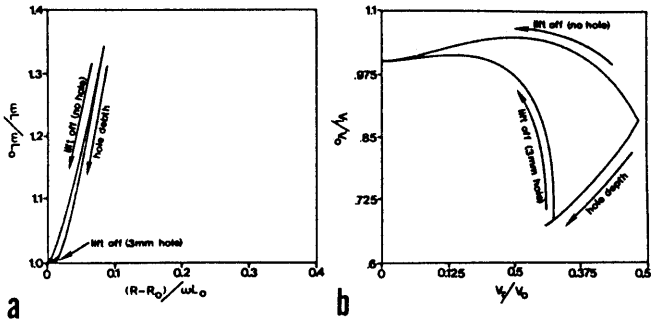

Fig. 7. Finite element prediction of normalized impedance and induced voltage due to lift off and hole depth change (defect). a) 4 mm single coil and b) double coil probe.

EXPERIMENTAL VERIFICATION

To verify the results presented above, a 30 mm diameter coil and a 4 mm diameter coil were constructed to form a double probe, while each coil could also be used separately as an absolute probe. Fig. 8 shows experimental results giving the normalized rates of change of both the impedance of single coil probes and the induced voltage of a double coil probe. In this figure, subscript '0' means zero lift off and subscript 'a' means that the coils are in air (far from the material). This shows, similar to the finite element results in Fig. 4, that potentially, the double probe has a larger range of measurements.

Fig. 9 shows the normalized impedance and voltage locus for a double probe. Although this is somewhat different than the results in Fig. 7 (due to uncertainty about the materials permeability and conductivity and fabrication errors), the same basic relations exist. In the case of the double coil the phase difference is larger between the lift off curve and the defect signal.

CONCLUSIONS

The results presented here clearly show the superiority of the double coil arrangement over the single coil (absolute probe) for such important measurements as lift off and corrosion or defect depth. Better linearity, larger sensitivity and significantly larger range of measurements are achieved. Moreover, in the case of defect detection by surface probes, the noise generated by lift off variations can be easily suppressed if double coil probes are used. The finite element method as a tool for probe design and for numerical experiments is also demonstrated. It is clear that any

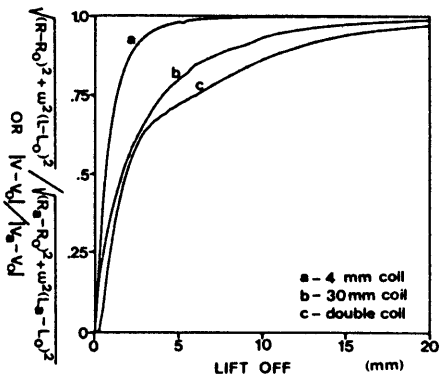

Fig. 8. Experimental impedance and induced voltage curves due to lift off.

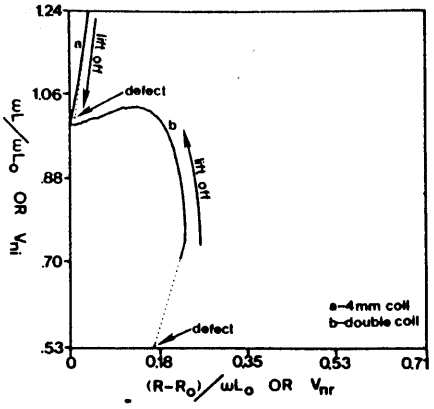

Fig. 9. Experimental, normalized impedance and induced voltage due to lift off and hole depth change (defect). A single hole is represented.

double coil probe, as is the case with any eddy current probe has to be optimized for the application for which it is designed. The finite element method is a powerful tool especially suited for such calculations.

REFERENCES

1. R. Palanisamy and W. Lord, "Finite element modeling of electromagnetic NDT phenomena," IEEE Transactions on Magnetics, Vol. MAG-15, No. 6, November 1979, pp. 1479-1481.
2. N. Ida, K. Betzold and W. Lord, "Finite element modeling of absolute eddy current probe signals," Journal of Nondestructive Evaluation, Vol. 3, No. 3, 1982, pp. 147-154.
3. N. Ida, R. Palanisamy and W. Lord, "Eddy current probe design using finite element analysis," accepted for publication in Materials Evaluation (Nov. 1983).

Review of Progress in QUANTITATIVE NONDESTRUCTIVE EVALUATION

Volume 3A

Edited by
Donald O. Thompson
Ames Laboratory (USDOE)
Iowa State University
Ames, Iowa
and
Dale E. Chimenti
Materials Laboratory
Air Force Wright Aeronautical Laboratories
Wright-Patterson Air Force Base
Dayton, Ohio

PLENUM PRESS • NEW YORK AND LONDON